THE UNIVERSITY of EDINBURGH

Edinburgh Research Explorer

Sound velocity of liquid Fe-Ni-S at high pressure

Citation for published version:
Kawaguchi, SI, Nakajima, Y, Hirose, K, Komabayashi, T, Ozawa, H, Tateno, S, Kuwayama, Y, Tsutsui, S & Baron, AQR 2017, 'Sound velocity of liquid Fe-Ni-S at high pressure', *Journal of Geophysical Research. Solid Earth*. https://doi.org/10.1002/2016JB013609

Digital Object Identifier (DOI):
10.1002/2016JB013609

Link:
Link to publication record in Edinburgh Research Explorer

Document Version:
Publisher's PDF, also known as Version of record

Published In:
Journal of Geophysical Research. Solid Earth

General rights
Copyright for the publications made accessible via the Edinburgh Research Explorer is retained by the author(s) and / or other copyright owners and it is a condition of accessing these publications that users recognise and abide by the legal requirements associated with these rights.

Take down policy
The University of Edinburgh has made every reasonable effort to ensure that Edinburgh Research Explorer content complies with UK legislation. If you believe that the public display of this file breaches copyright please contact openaccess@ed.ac.uk providing details, and we will remove access to the work immediately and investigate your claim.

Download date: 06. May. 2023

Sound velocity of liquid Fe–Ni–S at high pressure

Saori I. Kawaguchi[1,2,3], Yoichi Nakajima[4,5], Kei Hirose[2], Tetsuya Komabayashi[1,6], Haruka Ozawa[2,7], Shigehiko Tateno[2,7], Yasuhiro Kuwayama[8], Satoshi Tsutsui[3], and Alfred Q. R. Baron[3,4]

[1]Department of Earth and Planetary Sciences, Tokyo Institute of Technology, Tokyo, Japan

[2]Earth-Life Science Institute, Tokyo Institute of Technology, Tokyo, Japan

[3]Japan Synchrotron Radiation Research Institute, SPring-8, Hyogo, Japan

[4]Materials Dynamics Laboratory, RIKEN SPring-8 Center, RIKEN, Hyogo, Japan

[5]Priority Organization for Innovation and Excellence, Kumamoto University, Kumamoto, Japan

[6]School of GeoSciences and Centre for Science at Extreme Conditions, University of Edinburgh, Edinburgh, UK

[7]Institute for Planetary Materials, Okayama University, Tottori, Japan

[8]Geodynamics Research Center, Ehime University, Ehime, Japan

Correspondence to:

S. I. Kawaguchi

sao.kawaguchi@spring8.or.jp

Y. Nakajima

yoichi@kumamoto-u.ac.jp

Key Points:

- The sound velocity of liquid $Fe_{47}Ni_{28}S_{25}$ was measured up to 52 GPa.
- Extrapolation of measurements and comparison with seismic models suggest the presence of 5.8–7.5 wt.% sulfur in the Earth's outer core.

This article has been accepted for publication and undergone full peer review but has not been through the copyediting, typesetting, pagination and proofreading process which may lead to differences between this version and the Version of Record. Please cite this article as doi: 10.1002/2016JB013609

© 2017 American Geophysical Union. All rights reserved.

Accepted Article

Abstract

The sound velocity of liquid $Fe_{47}Ni_{28}S_{25}$ and $Fe_{63}Ni_{12}S_{25}$ was measured up to 52 GPa/2480 K in externally-resistance-heated and laser-heated diamond-anvil cells (DACs) using high-resolution inelastic X-ray scattering. From these experimental data, we obtained the elastic parameters of liquid $Fe_{47}Ni_{28}S_{25}$, K_{S0} = 96.1 ± 2.7 GPa and K_{S0}' = 4.00 ± 0.13, where K_{S0} and K_{S0}' are the adiabatic bulk modulus and its pressure derivative at 1 bar, when the density is fixed at ρ_0 = 5.62 ± 0.09 g/cm^3 for 1 bar and 2000 K. With these parameters, the sound velocity and density of liquid $Fe_{47}Ni_{28}S_{25}$ were calculated to be 8.41 ± 0.17 km/s and 8.93 ± 0.19 to 9.10 ± 0.18 g/cm^3, respectively, at the core mantle boundary (CMB) conditions of 135 GPa and 3600−4300 K. These values are 9.4 % higher and 17–18 % lower than those of pure Fe respectively. Extrapolation of measurements and comparison with seismological models suggest the presence of 5.8–7.5 wt.% sulfur in the Earth's outer core if it is the only light element.

1. Introduction

The Earth's liquid outer core is composed mainly of iron, but includes a substantial amount of light elements. The density deficit of the outer core relative to pure iron is estimated to be 5-–10%, depending on temperature [e.g., *Anderson and Isaak*, 2002]. Shock compression experiments performed by *Brown and McQueen* [1986] found that the sound velocity of pure liquid iron is about 3% slower than that of the material in the outer core. Such deviations of the density and sound velocity of liquid iron from seismologically observed values are reconciled with the presence of light elements in the core. Sulfur has been considered a

© 2017 American Geophysical Union. All rights reserved.

Accepted Article

possible light element because it is commonly found in meteorites [e.g., *Wasson*, 1974]. In addition, sulfur is depleted in the silicate Earth compared to other elements with similar volatility [*Palme and O'Neil*, 2013], implying that missing sulfur might reside in the core [*Rama Murthy and Hall*, 1970; *Dreibus and Palme*, 1996].

The sound velocity of liquid Fe–S alloy is important to examine the presence of sulfur in the core. Previous shock compression experiments on liquid Fe–S–O alloys to 230 GPa by *Huang et al.* [2011] indicated that a S-rich but O-poor liquid Fe alloy is consistent with both the velocity and density of the outer core. Ultrasonic wave measurements in a large-volume press also reported the sound velocity of liquid Fe–S alloys, although the pressure range examined was limited to below 8 GPa [*Jing et al.*, 2014; *Nishida et al*., 2016]. Calculations [*Badro et al*., 2014; *Umemoto et al.*, 2014] suggest that liquid Fe–S is not consistent with both the density and velocity of the Earth's outer core.

Recently, sound velocity measurements via inelastic X-ray scattering (IXS) have been extended to liquid Fe alloy at high pressures and high temperatures, approaching conditions in the outer core [*Nakajima et al.*, 2015]. Here, we use this technique to measure the velocity of liquid $Fe_{47}Ni_{28}S_{25}$ alloys in a DAC up to 52 GPa and $T \leq 2480$ K. The amount of sulfur in the Earth's outer core is discussed based on these new data on the velocity and density of liquid alloys.

Accepted Article

© 2017 American Geophysical Union. All rights reserved.

2. Experimental Methods

The sound velocity, equivalent to compressional wave (P-wave) velocity, of liquid $Fe_{46.5}Ni_{28.5}S_{25}$ (hereafter labeled as $Fe_{47}Ni_{28}S_{25}$) and $Fe_{63}Ni_{12}S_{25}$ was determined via high-resolution IXS measurements at beamline BL35XU of the SPring-8 synchrotron facility [*Baron et al.*, 2000]. High-pressure and -temperature (*P-T*) conditions were generated by using an externally-resistance-heated DAC (EHDAC) or a laser-heated DAC (LHDAC) (Table 1) using methods similar to described in *Komabayashi et al.* [2015] and Nakajima *et al.* [2015], respectively. Samples were compressed with flat diamond anvils with a 300 or 450 μm culet size to a pressure of interest before heating. The chemical compositions of starting specimens were $Fe_{47}Ni_{28}S_{25}$ and $Fe_{63}Ni_{12}S_{25}$ in atomic ratio. We used Ni-rich samples relative to the proposed composition for the Earth's core [*McDonough and Sun*, 1995] in order to lower melting temperatures, which facilitates melting, in particular in an EHDAC. They were pre-synthesized as single-phase solid $Fe_{47}Ni_{28}S_{25}$ and $Fe_{63}Ni_{12}S_{25}$ using a multi-anvil apparatus at 25 GPa and used for runs #1 and #4–7. A powder mixture of Fe, Ni, and FeS with $Fe_{47}Ni_{28}S_{25}$ composition was employed in runs #2 and #3. The compositions of these starting samples were confirmed by a field-emission-type electron-probe micro-analyzer (FE-EPMA). The samples were about 20 μm and 40–50 μm thick for laser- and resistance-heated DACs, respectively, and 80–130 μm in diameter. They were loaded into a 100–150 μm hole in a pre-indented rhenium gasket. For run #5–7 single-crystal sapphire disks were placed inside the DAC to thermally and chemically isolate the sample from the diamond anvils. FE-EPMA analysis of a recovered sample did not detect carbon in quenched molten metal. In run #4, an Al_2O_3 inner gasket was adopted. Pressure at room temperature was determined by the Raman shift of the diamond anvils [*Akahama and Kawamura*, 2004].

© 2017 American Geophysical Union. All rights reserved.

Accepted Article

We consider thermal pressure to be +5% per 1000 K [*Nomura et al.*, 2014]. The uncertainty in pressure was estimated to be not more than 10%. In separate experiments with a sample configuration similar to the present one, thermal pressures were measured at 15 and 40 GPa, based on in-situ XRD observations of fcc Fe [*Tsujino et al.*, 2013]. Our results are consistent with the thermal pressure correction employed in that study.

In the EHDAC experiments (run #1−4), the samples were heated by a resistive heating furnace made of a platinum wire shaped into a coil [*Komabayashi et al.*, 2015]. In run #5‑7, we used a double-sided laser-heating system [*Nakajima et al.*, 2015]. The heating spot on the sample was 40 to 60 μm, which was more than double the size of a probed X-ray beam. To reduce the background in the IXS spectra from air scattering in these measurements at low momentum transfers, the DACs in both resistance- and laser-heated experiments were placed into vacuum chambers. The temperature was measured by an R-type thermocouple for EHDAC and by a spectroradiometric method for LHDAC. Temperature fluctuation during resistance- and laser-heating was less than 50 K and 10%, respectively. Melting of a sample was judged from the disappearance of X-ray diffraction (XRD) peaks from solid alloy collected with an X-ray flat panel detector [*Fukui et al.*, 2013].

IXS measurements were carried out in a Si(999) backscattering geometry using 17.79 keV X-rays with an over-all with energy resolution of about 2.8 meV. For EHDAC (run# 1–4), the incident X-ray beam was < 90 μm × 80 μm (full width at half maximum, FWHM). For LHDAC (run #5–7), the beam was focused to ~17 μm × 17 μm area by a Kirkpatrick-Baez focusing mirror optics [*Ishikawa et al.*, 2013]. At each *P-T* condition, IXS spectra were collected at different momentum transfers (*Q*) using an array of twelve independent spherical

© 2017 American Geophysical Union. All rights reserved.

Accepted Article

analyzer crystals. The *Q* range was 3.2‐6.6 nm^{-1} with resolution of ~0.4 nm^{-1} full width. A typical uncertainty in the Q determination was < ±0.02 nm^{-1} in the present set-up. Spectra were measured over an energy range less than or up to -30 to 40 meV with exposure time of 1‐4 hours. The uncertainty in the energy calibration was ~0.5% [*Fukui et al.*, 2008].

3. Results

We investigated seven liquid (Fe,Ni)‐S samples in a pressure range from 10 to 52 GPa (Table 1). These experimental *P-T* conditions are compared to the eutectic melting curves of the Fe-S and Fe–Ni–S systems in Figure 1 [e.g., *Fei et al*., 1997, 2000; *Morard et al.*, 2008; *Mori et al*., 2017]. We determined the melting point of a sample by the disappearance of the solid sample peaks in XRD patterns. Figure 2 shows typical XRD patterns during and after heating at 32 GPa in the LHDAC. In heating from room temperature to below 1800 K, we observed a change in two-dimensional XRD image from Debye-Scherrer rings to spotty Bragg-peaks, indicating the grain growth of the solid $(Fe,Ni)_3S$ phase. Upon further heating, the diffraction peaks from solid $(Fe,Ni)_3S$ disappeared, indicating a molten state of the sample. At pressures below 20 GPa, the $Fe_{47}Ni_{28}S_{25}$ and $Fe_{63}Ni_{12}S_{25}$ sample decomposed into a mixture of fcc Fe-Ni and (Fe,Ni)S around 900 K before melting. We confirmed a fully molten state of the sample before and after collecting IXS data. The sample Bragg peaks reappeared when the temperature was lowered. The present experimental conditions were well above the Fe–S and Fe–Ni–S eutectic melting temperatures (Figure 1). The compositions of liquids in the LHDAC experiments could have been different from the starting composition but close to a eutectic composition at each pressure. If this is the case, the sulfur content of the liquid may

© 2017 American Geophysical Union. All rights reserved.

Accepted Article

have changed from 30 to 20 at.% with increasing pressure in the present study from 10 to 52 GPa rather than being the nominal 25 at.% [*Fei et al*., 1997, 2000; *Stewart et al*., 2007; *Morard et al*., 2008; *Mori et al*., 2017].

Typical IXS spectra of liquid samples obtained at 51.6 GPa/2480 K during laser heating and at 20.3 GPa/1450 K with resistance heating are shown in Figure 3. The peak at zero energy transfer is from quasi-elastic contributions. The acoustic (LA) phonon modes appear as matching Stokes/anti-Stokes peak pairs at positive/negative energy transfers. The LA peaks of the sample are the lowest energy clear peak; spectra at small Q show an additional peak at high energy from the diamond TA modes. The phonon peaks were fit with a damped harmonic oscillator (DHO) model function [*Fåk and Doner*, 1997], convolved with the measured resolution function.

The phonon dispersion for all the runs is shown in Figure 4. The compressional (P-wave) velocity (V_P), corresponds to a longitudinal acoustic velocity in the long wavelength (small Q), limit. This was determined by making a linear fit to the data for $Q < 3.5$ nm^{-1}. This linear fit use the error bars in the peak energies as determined from the fits to the spectra. The low Q data, only, was used to avoid possible effects of "positive dispersion" [see *Scopigno*, 2005, *Hosokawa et al.*, 2008a, 2008b].

These results demonstrate that V_P of liquid $Fe_{47}Ni_{28}S_{25}$ increased from 4.71 ± 0.43 km/s at 9.5 GPa to 6.40 ± 0.61 km/s at 52 GPa (Table 1). The V_P of liquid $Fe_{47}Ni_{28}S_{25}$ and $Fe_{63}Ni_{12}S_{25}$ is plotted as a function of pressure in Figure 5. It is slower by 11 % than that of solid Fe_3S at 2000 K at a given pressure, which is calculated, on the basis of Birch's law [*Birch*, 1961],

© 2017 American Geophysical Union. All rights reserved.

Accepted Article

from the sound velocity of solid Fe_3S at room temperature [*Kamada et al.*, 2014] combined with the temperature effect on its density [*Seagle et al.*, 2006].

4. Sound Velocity and density of Liquid Fe–Ni–S at High *P-T*

4.1. Temperature Effect on Sound Velocity

All data are plotted on a single P-V_P curve (Figure 5), showing small temperature dependence. This is consistent with a large body of work, suggesting the effect of temperature on V_P of liquid iron alloy is small for $T \leq 2480$ K. Previous high-pressure ultrasonic measurements of liquid Fe–S alloys reported a negligible temperature effect on their sound velocities over 1500 K [*Jing et al.*, 2014; *Nishida et al*., 2016]. A temperature effect on the V_P of liquid Fe–C was not found in the recent laser-heated DAC study performed by *Nakajima et al*. [2015]. Theoretical calculations at core pressures have also suggested that the sound velocities of liquid Fe and Fe–S alloys are not sensitive to temperature [*Vočadlo et al*., 2003; *Ichikawa et al*., 2014; *Umemoto et al*., 2014].

In contrast, large positive temperature dependence was observed in $Fe_{86}S_{16}$ at 1 bar [*Nasch et al*., 1997]. Depending on the sulfur content, solid Fe–S alloys are known to be semi-metal [*Kusaba et al.*, 1997], suggesting that sulfur-rich liquid Fe might be semi-metallic rather than metallic at 1 bar. Indeed, positive or anomalous temperature dependence has been observed in liquid semi-metals such as silicon and germanium at ambient pressure [*Hayashi et al.*, 2007]. The positive temperature effect found by *Nasch et al.* [1997] is possibly a result of the semi-metallic nature at ambient pressure. Such semi-metallic feature disappears upon

© 2017 American Geophysical Union. All rights reserved.

Accepted Article

transition to a compact structure in liquid FeS above 1 GPa [*Nishida et al*., 2011] and in liquid Fe containing ~30 at.% S at 13–17 GPa [*Morard et al.*, 2007].

4.2. Pressure Dependence of Sound Velocity

The present results, all above 10 GPa, show a different pressure slope than ultrasonic measurements carried out below 8 GPa [*Jing et al*., 2014; *Nishida et al*., 2016] (see Figure 5). The pressure dependence we observe here is more gentle, similar to what has been observed previously for liquid iron and alloys [*Anderson and Ahrens*, 1994]. Given this, and the rather large difference between the results of Jing et al. ($Fe_{83.8}S_{16.2}$) and Nishida et al. ($Fe_{80}S_{20}$), and several previous reports pointing to structural [*Nishida et al*., 2011; *Morard et al.*, 2007] and electronic [*Kusaba et al.*, 1997] phase transitions in the Fe–S system, we expect the differences in slope are due to phase changes of the melt in the low-pressure region.

The present experimental data was measured in conditions closer to those of the Earth's core than previous work, and provides improved constraints on the pressure dependence of the sound velocity there. We employed the adiabatic Murnaghan equation of state (EoS) [e.g., *Jing et al.*, 2014]:

$$\rho(P) = \rho_0 \left[1 + P\left(\frac{K'_{S0}}{K_{S0}}\right)\right]^{1/K'_{S0}}, \quad (1)$$

where ρ, K_S, and $K_S{}'$ are the density, adiabatic bulk modulus, and its pressure derivative, respectively. Zero subscripts denote values at 1 bar and T_0 (temperature at 1 bar isentropic to T at high P). The P-wave velocity is written as:

© 2017 American Geophysical Union. All rights reserved.

$$V_P = \sqrt{\frac{K_S + 4G/3}{\rho}}\ , \qquad (2)$$

where G is shear modulus. For the liquid, the shear modulus can be neglected, and so the Murnaghan EoS (Eq. 1) becomes:

$$V_P = \sqrt{\frac{K_{S0}}{\rho_0}}\left[1 + P\left(\frac{K'_{S0}}{K_{S0}}\right)\right]^{\left(1-1/K_{S0}\right)/2}. \qquad (3)$$

ρ_0 of liquid $Fe_{47}Ni_{28}S_{25}$ was estimated to be 5.62 ± 0.09 g/cm^3 at 1 bar and 2000 K based on the EoSs for Fe [*Anderson and Ahrens*, 1994] and FeS [*Nishida et al*., 2011] assuming an ideal mixing. The uncertainty was derived from the uncertainties in the EoS parameters for liquid Fe and Fe–S. The effect of Ni was taken into account by following *Brillo and Egry* [2004]. The EoS parameters for liquid FeS were from data at pressures above 0.5 GPa, where a structural transition occurs in liquid [*Nishida et al*., 2011]. As we discussed above, we consider that V_P is not directly sensitive to temperature but ρ is temperature dependent. With a fixed 1 bar density, the fitting of Eq. 3 to the present P-V_P data yields K_{S0} = 96.1 ± 2.7 GPa and K_{S0}' = 4.00 ± 0.13 for liquid $Fe_{47}Ni_{28}S_{25}$ at 2000 K (Table 2).

4.3. Effect of Nickel

We find the effect of nickel on the sound velocity of liquid Fe–S alloys to be very small. The sample used in run #1 included 63 at.% Fe and 12 at.% Ni, whereas others contained 48 at.% Fe and 27 at.% Ni. The velocity obtained for the former is consistent with the P-V_P relation for the latter (Figure 5). This is consistent with sound velocity measurements of liquid Fe–Ni alloys at 1 bar [*Nasch and Manghnani*, 1998], which showed that elastic properties are very

© 2017 American Geophysical Union. All rights reserved.

Accepted Article

similar for liquid Fe–Ni alloys with nickel contents ranging from 0 to 34 at.%. A similarly small effect of Ni on elastic parameters was also reported for solid Fe–Ni alloys [*Mao et al*., 1990].

The small impact of Ni substitution is confirmed by considering Eq. (3) Changing ρ_0 from that of $Fe_{47}Ni_{28}S_{25}$ to that of $Fe_{63}Ni_{12}S_{25}$ (as given by *Brillo and Agry*, 2004) leads to the difference in sound velocity by only ~1.2%. Similar considerations suggest the velocities of liquid $Fe_{47}Ni_{28}S_{25}$ and $Fe_{63}Ni_{12}S_{25}$ are lower than that of Ni-free $Fe_{75}S_{25}$ by 0.8–1.8 %. These fall within the error bars of the present measurements.

4.4. Liquid Density Profiles

The *P*-ρ relation is given by Eq. (1) along an adiabatic temperature profile (solid pink curve in Figure 6). The adiabatic temperature gradient is written as $(\partial \ln T / \partial \ln \rho) = \gamma$, where γ is the Grüneisen parameter. We assume γ is simply related to density as $\gamma = \gamma_0 \times (\rho_0/\rho)$. We use $\gamma_0 =$ 1.74 from the Grüneisen parameter of pure liquid iron at 1 bar and 1811 K [*Anderson and Ahrens*, 1994]. Then, the adiabatic temperature profile can be described as:

$$T = T_0 exp\left[\gamma_0\left(1 - \frac{\rho_0}{\rho}\right)\right]. \quad (4)$$

Note that ρ_0 is the 1 bar density, not at 300 K, but at T_0. For the present sample $Fe_{47}Ni_{28}S_{25}$, ρ_0 at each temperature can be calculated from literature data [*Anderson and Ahrens*, 1994; *Brillo and Egry*, 2004; *Nishida et al.*, 2011]. Assuming that velocity profile is independent of temperature, the high-pressure isothermal density profile of liquid $Fe_{47}Ni_{28}S_{25}$ is obtained and

© 2017 American Geophysical Union. All rights reserved.

Accepted Article

illustrated in Figure 6.

Previous experiments performed by *Sanloup et al*. [2000] and *Morard et al*. [2013] reported the isothermal density profiles of liquid $Fe_{83.8}S_{16.2}$ at 1770 K and $Fe_{76}Ni_4S_{19}$ at 2600 K, respectively. Here we calculated the densities of those two liquids using data from the present study for liquid $Fe_{47}Ni_{28}S_{25}$ and of pure Fe [*Anderson and Ahrens,* 1994], assuming a linear relation between these two (Figure 6). The effect of Ni was included by changing ρ_0 based on *Brillo and Agry* [2004]. Our estimate for liquid $Fe_{76}Ni_4S_{19}$ agrees very well with the measurements above 28 GPa by *Morard et al*. [2013] using an X-ray diffuse scattering signal from liquid. On the other hand, our estimate is not consistent with low-pressure measurements ($\leq$ 6.2 GPa) by *Sanloup et al*. [2000]. This may be the result of the structural transition as discussed above.

5. Implications for the Core Composition of Earth and, eventually, Mars

According to seismological observations (Preliminary Reference Earth Model, PREM) [*Dziewonski and Anderson*, 1981] and shock compression experiments [e.g., *Anderson and Ahrens*, 1994], V_P in the outer core is higher than that of pure iron. In order to examine the presence of sulfur in the Earth's liquid core, we extrapolate the present sound velocity and density data for liquid $Fe_{47}Ni_{28}S_{25}$ to core pressures, using elastic parameters obtained above (Table 2). The uncertainties in extrapolated velocity and density were estimated by propagating the uncertainties in elastic parameters listed in Table 2. We also added a possible systematic uncertainty due to the use of the Murnaghan EoS rather than a higher ordered EoS such as the Birch-Murnaghan EoS [*Nakajima et al*, 2015]. Those uncertainties in velocity and

© 2017 American Geophysical Union. All rights reserved.

Accepted Article

density are illustrated in Figures 7 and 8. The calculated density based on the Murnaghan EoS is in reasonable agreement with the density measured to 100 GPa by *Morard et al*. [2013], which supports the validity of the present extrapolation to at least 100 GPa.

The extrapolated sound velocity for liquid $Fe_{47}Ni_{28}S_{25}$ is approximately consistent with theoretical calculations on $Fe_{75}S_{25}$ reported by *Badro et al.* [2014] and *Umemoto et al.* [2014] (Figure 7). Figure 8 shows our calculated density along adiabatic temperature profiles with T_0 = 1876 K and 2212 K, which corresponds to the temperatures at CMB, T_{CMB} = 3600 K and 4300 K, respectively (Figure S1). The sound velocity and density of liquid $Fe_{47}Ni_{28}S_{25}$ are found to be 8.41 ± 0.17 km/s and 8.93 ± 0.19 to 9.10 ± 0.18 g/cm^3, respectively, at 135 GPa and 3600−4300 K.

We compare our results with shock compression results for the density of liquid pure Fe [*Anderson and Ahrens,* 1994] and liquid $Fe_{81}S_{19}$ [*Huang et al.*, 2013] (Figure 8). The density of liquid $Fe_{47}Ni_{28}S_{25}$ calculated here is 17% less than that of pure Fe in the core pressure range. Compared with that of $Fe_{81}S_{19}$, $Fe_{47}Ni_{28}S_{25}$ is less dense by 11% at 135 GPa and by 8% at 200 GPa. When recalculating the $Fe_{81}S_{19}$ density based on additive law by mixing the densities of $Fe_{47}Ni_{28}S_{25}$ and Fe [*Anderson and Ahrens*, 1994], our results are still lower by 7% than that of *Huang et al*. [2013]. On the other hand, our results agree with those of *Morard et al*. [2013] within uncertainty. The origin of the difference is not clear.

Finally, we consider the amount of sulfur in the Earth's liquid core on the basis of the present study. First of all, the V_P profile of the PREM is best explained with 5.8 ± 2.5 wt.% S ($Fe_{84.9}Ni_{5.4}S_{9.7}$ in atomic ratio) over the whole outer core (Figure 7), if we assume that the

© 2017 American Geophysical Union. All rights reserved.

Accepted Article

substitution of iron by nickel does not affect the velocity. In addition, when considering 5.4 at.% Ni, the PREM density profile is well explained with 6.5 ± 0.7 to 7.5 ± 0.8 wt.% S ($Fe_{83.7}Ni_{5.4}S_{10.9}$–$Fe_{82.2}Ni_{5.4}S_{12.4}$) depending on the CMB temperature ranging from 3600 to 4300 K (Figure 8). We therefore conclude that the density and velocity of the outer core suggest the presence of 5.8–7.5 wt.% S if sulfur is the only light element. The sulfur content obtained in this study is lower than the ~10 wt.% from previous density measurements of liquid Fe–Ni–S [*Morard et al.*, 2013]. However, such estimate is recalculated to be 7.5–7.7 wt.% when employing the density of liquid Fe from *Anderson and Ahrens* [1994] same as used here.

It has been suggested that the bulk Earth contains only a limited amount of sulfur because of its high volatility. Considering zinc is an absolute lithophile element and similar in volatility to sulfur, *Dreibus and Palme* [1996] estimated on the basis of S/Zn ratio in the silicate mantle that the sulfur content in the bulk Earth is only 0.6%. This gives the maximum sulfur concentration in the core to be 1.7 wt.%. However, recent metal–silicate partitioning experiments [*Corgne et al*., 2008] indicated that zinc is not highly lithophile at high pressure, suggesting that the core may include much more sulfur. It is therefore possible from geochemical point of view that 5.8–7.5 wt.% sulfur is present in the liquid outer core as estimated above.

The present experimental data are relevant to understanding to composition of the Martian core, as it is widely believed to be sulfur rich [e.g., *Dreibus and Wänke*, 1985]. According to the Mars composition models derived from SNC meteorite [e.g., *Dreibus and Wänke*, 1987], the Martian mantle is depleted in chalcophile elements and enriched in volatile and

© 2017 American Geophysical Union. All rights reserved.

Accepted Article

moderately siderophile elements compared to the Earth's mantle. It suggests that the Mars was under more oxidized conditions during accretion and core formation [*Halliday et al.*, 2001; *Rai et al.*, 2013]. In oxidative conditions, sulfur tends to be more readily incorporated into iron than silicate [*Francis*, 1990]. Therefore, it has been considered that sulfur is the predominant light element in the Martian core. Figures 9a and b show the sound velocity and isothermal density profiles (at 1500, 1900, and 2300 K) of Fe-10 wt.%S ($Fe_{77.0}Ni_{6.8}S_{16.2}$) and Fe-16 wt.%S ($Fe_{68.5}Ni_{6.5}S_{25}$) in the Martian core pressure range (20–50 GPa, *Tsujino et al*. [2013] and references therein) assuming 7.6 wt.%Ni [*Dreibus and Wänke*, 1987]. Since the present data extends to more than 19 GPa [e.g., *Rivoldini et al*., 2011], it is more relevant to discuss the Martian core composition than that of previous studies below 8 GPa [*Jing et al.*, 2014; *Nishida et al.*, 2016]. As discussed above, elastic properties and thus sound velocity at lower pressures are different from those above 10 GPa because of the changes in liquid structure and electronic properties [*Morard et al.*, 2007; *Nishida et al*., 2011]. The present results will therefore be useful to investigate the amount of sulfur in the Martian core, when its seismic data becomes available from upcoming explorations.

6. Summary and Conclusions

We have measured the sound velocity of liquid $Fe_{47}Ni_{28}S_{25}$ and $Fe_{63}Ni_{12}S_{25}$ to 52 GPa using high-resolution inelastic X-ray scattering to investigate samples in both externally-resistance-heated and laser-heated DACs. The P-wave velocity is determined to be 6.4 ± 0.3 km/s at 52 GPa, and to be insensitive to temperature within 1.5% at $T \leq 2480$ K. The pressure derivative of the sound velocity of liquid $(Fe,Ni)_{75}S_{25}$ is found to be smaller than

© 2017 American Geophysical Union. All rights reserved.

Accepted Article

that of previous studies at lower pressures [*Jing et al*., 2014; *Nishida et al*., 2016], possibly due to a transition to a compact liquid structure occurring just above the pressure of the earlier works [see *Morard et al*., 2007; *Nishida et al*., 2011]. The effect of nickel content on the sound velocity, after correction for the density change [*Brillo and Egry*, 2004] was observed to be < 1.5%. We extrapolate our data to the conditions of the outer core using also literature data on thermoelastic properties [*Anderson and Ahrens*, 1994; *Brillo and Egry*, 2004; *Nishida et al.*, 2011]. Extrapolation of measured sound velocity and density and comparison with seismological models suggest that the composition of Earth's outer core may be Fe + 5.8–7.5 wt.% S ($Fe_{84.9}Ni_{5.4}S_{9.7}$–$Fe_{82.2}Ni_{5.4}S_{12.4}$ in atomic ratio) if sulfur is the only light alloying component.

Acknowledgments

Data supporting Figure 5 is available as in Table 1. We thank H. Fukui and H. Uchiyama for their advice and technical support. We also thank K. Umemoto, Y. Ohishi and S. Kawaguchi for their fruitful comments. A part of thin sapphire discs used in experiments was supplied by Engis Japan Co. Comments from M. Walter and anonymous referees were helpful to improve the manuscript. Inelastic X-ray scattering measurements were performed at SPring-8 (proposal no. 2011B1336, 2012A1237, 2012B1356, 2012B1159, 2013A1438, 2013A1541, 2013B1154, 2013B1407, 2014A1368, 2014B1271, and 2014B1536). The data for this paper are available by contacting the corresponding author at sao.kawaguchi@spring8.or.jp.

References

Akahama, Y., and H. Kawamura (2004), High-pressure Raman spectroscopy of diamond anvils to 250 GPa: method for pressure determination in the multimegabar pressure range,

© 2017 American Geophysical Union. All rights reserved.

Accepted Article

J. Appl. Phys., *96*, 3748–3751, doi:10.1063/1.1778482.

Anderson, W. W., and T. J. Ahrens (1994), An equation of state for liquid iron and implications for the Earth's core, *J. Geophys. Res.*, *99*, 4273–4284, doi:10.1029/93JB03158.

Anderson, O. L., and D. G. Isaak (2002), Another look at the core density deficit of Earth's outer core, *Phys. Earth Planet. Inter.*, *131*, 19–27, doi:10.1016/S0031-9201(02)00017-1.

Badro, J., A. S. Cote, and J. P. Brodholt (2014), A seismologically consistent compositional model of Earth's core, *Proc. Natl. Acad. Sci.*, *111*, 7542–7545, doi:10.1073/pnas.1316708111.

Baron, A. Q. R., Y. Tanaka, S. Goto, K. Takeshita, T. Matsushita, and T. Ishikawa (2000), X-ray scattering beamline for studying dynamics, *J. Phys. Chem. Solids*, *61*, 461–465, doi:10.1016/S0022-3697(99)00337-6.

Birch, F. (1961), The velocity of compressional waves in rocks to 10 kilobars, part 2, *J. Geophys. Res.*, *66*, 2199–2224.

Brillo, J, and I. Egry (2004), Density and excess volume of liquid copper, nickel, iron, and their binary alloys, *Zeitschrift für Metallkunde*, *95*, 691–697.

Brown, J. M., and R. G. McQueen (1986), Phase transitions, Grüneisen parameter, and elasticity for shocked iron between 77 GPa and 400 GPa, *J. Geophys. Res.*, *91*, 7485, doi:10.1029/JB091iB07p07485.

Corgne, A., S. Keshav, B. J. Wood, W. F. McDonough, and Y. Fei (2008), Metal-silicate partitioning and constraints on core composition and oxygen fugacity during Earth accretion, *Geochim. Cosmochim. Acta*, *72*, 574–589, doi:10.1016/j.gca.2007.10.006.

Dreibus, G., and H. Palme (1996), Cosmochemical constraints on the sulfur content in the

© 2017 American Geophysical Union. All rights reserved.

Accepted Article

Earth's core, *Geochim. Cosmochim. Acta*, *60*, 1125–1130, doi:10.1016/0016-7037(96)00028-2.

Dreibus, G, and H. Wänke (1985), Mars, a volatile-rich planet, *Meteoritics*, *20*, 367–381.

Dreibus, G., and H. Wänke (1987), Volatiles on Earth and Mars: A comparison, *Icarus*, *71*(2), 225–240, doi:10.1016/0019-1035(87)90148-5.

Dziewonski, A. M., and D. L. Anderson (1981), Preliminary reference Earth model, *Phys. Earth Planet. Inter.*, *25*, 297–356.

Fei, Y., C. M. Bertka, and L. W. Finger (1997), High-pressure iron-sulfur compound, Fe_3S_2, and melting relations in the Fe–FeS system, *Science*, *275*, 1621–1623, doi:10.1126/science.275.5306.1621.

Fei, Y., J. Li, C. M. Bertka, and C. T. Prewitt (2000), Structure type and bulk modulus of Fe_3S, a new iron-sulfur compound, *Am. Mineral.*, *85*, 1830–1833.

Francis, R. D. (1990), Sulfide globules in mid-ocean ridge basalts (MORB), and the effect of oxygen abundance in Fe–S–O liquids on the ability of those liquids to partition metals from MORB and komatiite magmas, *Chem. Geol.*, *85*, 199–213.

Fukui, H., T. Katsura, T. Kuribayashi, T. Matsuzaki, A. Yoneda, E. Ito, Y. Kudoh, S. Tsutsui, and A. Q. R. Baron (2008), Precise determination of elastic constants by high-resolution inelastic X-ray scattering, *J. Synchrotron Radiat.*, *15*, 618–623, doi:10.1107/S0909049508023248.

Fåk, B., and B. Dorner (1997), Phonon line shapes and excitation energies, *Phys. B Condens. Matter*, *234–236*, 1107–1108, doi:10.1016/S0921-4526(97)00121-X.

Halliday, A. N., H. Wänke, J. L. Birck, and R. N. Clayton (2001), The accretion, composition and early differentiation of Mars, in Chronology and Evolution of Mars, edited by R.

© 2017 American Geophysical Union. All rights reserved.

Accepted Article

Kallenbach et al., pp. 197–230, Springer, Netherlands.

Hayashi M., H. Yamada, N. Nabeshima, and K. Nagata (2007), Temperature dependence of the velocity of sound in liquid metals of group XIV, *Inter. J. Thermophys.*, *28*, 83–96.

Hosokawa, S., M. Inui, K. Matsuda, D. Ishikawa, and A. Q. R. Baron (2008a), Damping of the collective modes in liquid Fe, *Phys. Rev. B*, *77*, 174203, doi: 10.1103/PhysRevB.77.174203.

Hosokawa, S., W.-C. Pilgrim, H. Sinn, and E. E. Alp (2008b), The possibility of transverse excitation modes in liquid Ga, *J. Phys.: Condens. Matter*, *20*, 114107-1-7 .

Huang, H., Y. Fei, L. Cai, F. Jing, X. Hu, H. Xie, L. Zhang, and Z. Gong (2011), Evidence for an oxygen-depleted liquid outer core of the Earth, *Nature*, *479*, 513–516, doi:10.1038/nature10621.

Huang, H., S. Wu, X. Hu, Q. Wang, X. Wang, and Y. Fei (2013), Shock compression of Fe–FeS mixture up to 204 GPa, *Geophys. Res. Lett.*, *40*, 687–691, doi:10.1002/grl.50180.

Ichikawa, H., T. Tsuchiya, and Y. Tange (2014), The P-V-T equation of state and thermodynamic properties of liquid iron, *J. Geophys. Res. Solid Earth*, *119*, 240–252, doi:10.1002/2013JB010732.

Ishikawa, D., H. Uchiyama, S. Tsutsui, H. Fukui, and A. Q. R. Baron (2013), Compound focusing for hard-x-ray inelastic scattering, *Proc. SPIE*, *8848*, 88480F, doi:10.1117/12.2023795.

Jing, Z., Y. Wang, Y. Kono, T. Yu, T. Sakamaki, C. Park, M. L. Rivers, S. R. Sutton, and G. Shen (2014), Sound velocity of Fe-S liquids at high pressure: implications for the Moon's molten outer core, *Earth Planet. Sci. Lett.*, *396*, 78–87, doi:10.1016/j.epsl.2014.04.015.

Kamada S., E. Ohtani, H. Fukui, T. Sakai, H. Terasaki, S. Takahashi, Y. Shibazaki, S. Tsutsui,

© 2017 American Geophysical Union. All rights reserved.

Accepted Article

A. Q. R. Baron, N. Hirao, and Y. Ohishi (2014), The sound velocity measurements of Fe_3S, *Am. Mineral.*, *99*, 98–251.

Komabayashi, T., J. Kato, H. Hirose, S. Tsutsui, S. Imada, Y. Nakajima, and A. Q. R. Baron (2015), Temperature dependence of the velocity–density relation for liquid metals under high pressure: implications for the Earth's outer core, *Am. Mineral*, *100*, 2602–2609, doi: 10.2138/am-2015-5294.

Kusaba, K., Y. Syono, T. Kikegawa, and O. Shimomura (1997), Structure of FeS under high pressure, *J. Phys. Chem. Solids*, *58*, 241–246, doi:10.1016/S0022-3697(96)00120-5.

Mao, H. K., Y. Wu, L. C. Chen, J. F. Shu, J. F., and A. P. Jephcoat, (1990), Static compression of iron to 300 GPa and $Fe_{0.8}Ni_{0.2}$ alloy to 260 GPa: implications for composition of the core, *J. Geophys. Res. Solid Earth*, *95*, 21737–21742.

McDonough, W. F., and S. S. Sun (1995), The composition of the Earth, *Chem. Geol.*, *120*, 223–253.

Morard, G., C. Sanloup, G. Fiquet, M. Mezouar, N. Rey, R. Poloni, and P. Beck (2007), Structure of eutectic Fe–FeS melts to pressures up to 17 GPa: implications for planetary cores, *Earth Planet. Sci. Lett.*, *263*, 128–139, doi:10.1016/j.epsl.2007.09.009.

Morard, G., D. Andrault, N. Guignot, C. Sanloup, M. Mezouar, S. Petitgirard, G. Fiquet (2008), In situ determination of Fe–Fe_3S phase diagram and liquid structural properties up to 65 GPa, *Earth Planet. Sci. Lett.*, *272*, 620–626, doi.org/10.1016/j.epsl.2008.05.028.

Morard, G., J. Siebert, D. Andrault, N. Guignot, G. Garbarino, F. Guyot, and D. Antonangeli (2013), The Earth's core composition from high pressure density measurements of liquid iron alloys, *Earth Planet. Sci. Lett.*, *373*, 169–178, doi:10.1016/j.epsl.2013.04.040.

Mori, Y., H. Ozawa, K. Hirose, R. Sinmyo, S. Tateno, G. Morard, and Y. Ohishi (2017),

© 2017 American Geophysical Union. All rights reserved.

Accepted Article

Melting experiments on Fe–Fe_3S system to 254 GPa, *Earth Planet. Sci. Lett.*, 464, 135–141, doi.org/10.1016/j.epsl.2017.02.021.

Nakajima, Y., S. Imada, K. Hirose, T. Komabayashi, H. Ozawa, S. Tateno, S. Tsutsui, Y. Kuwayama, and A. Q. R. Baron (2015), Carbon-depleted outer core revealed by sound velocity measurements of liquid iron–carbon alloy, *Nat. Commun.*, *6*, 8942, doi:10.1038/ncomms9942.

Nasch, P. M., and M. H. Manghnani (1998), Molar volume, thermal expansion, and bulk modulus in liquid Fe–Ni alloys at 1 Bar: Evidence for magnetic anomalies?, in Properties of Earth and Planetary Materials at High Pressure and Temperature, edited by M. H. Manghnani and T. Yagi, pp. 307–317, AGU, Washington, D. C.

Nasch, P., M. Manghnani, and R. Secco (1997), Anomalous behavior of sound velocity and attenuation in liquid Fe–Ni–S, *Science*, *277*, 219–221.

Nishida, K., E. Ohtani, S. Urakawa, A. Suzuki, T. Sakamaki, H. Terasaki, and Y. Katayama (2011), Density measurement of liquid FeS at high pressures using synchrotron X-ray absorption, *Am. Mineral.*, *96*, 864–868, doi:10.2138/am.2011.3616.

Nishida, K., A. Suzuki, H. Terasaki, Y. Shibazaki, Y. Higo, S. Kuwabara, Y. Shimoyama, M. Sakurai, M. Ushioda, E. Takahashi, T. Kikegawa, D. Wakabayashi, N. Funamori (2016), Towards a consensus on the pressure and composition dependence of sound velocity in the liquid Fe–S system, *Phys. Earth Planet. Inter.*, *257*, 230–239, doi:http://dx.doi.org/10.1016/j.pepi.2016.06.009.

Nomura, R., K. Hirose, K. Uesugi, Y. Ohishi, A. Tsuchiyama, A. Miyake, and Y. Ueno (2014), Low core–mantle boundary temperature inferred from the solidus of pyrolite, *Science*, *343*, 522–525.

© 2017 American Geophysical Union. All rights reserved.

Accepted Article

Palme, H., and H. O'Neill (2013), Cosmochemical estimates of mantle composition, in Treaties of Geochemistry, 2nd ed., edited by Holland and Karl Turekian, Elsevier Ltd, http://dx.doi.org/10.1016/B978-0-08-095975-7.00201-1.

Rai, N., and W. Van Westrenen (2013), Core–mantle differentiation in Mars, *J. Geophys. Res. Planets*, *118*, 1195–1203, doi:10.1002/jgre.20093.

Rama Murthy, V., and H. T. Hall (1970), The chemical composition of the Earth's core: possibility of sulphur in the core, *Phys. Earth Planet. Inter.*, *2*, 276–282, doi:10.1016/0031-9201(70)90014-2.

Rivoldini, A., T. Van Hoolst, O. Verhoeven, A. Mocquet, and V. Dehant (2011), Geodesy constraints on the interior structure and composition of Mars, *Icarus*, *213*, 451–472, doi:10.1016/j.icarus.2011.03.024.

Sanloup, C., F. Guyot, P. Gillet, G. Fiquet, M. Mezouar, and I. Martinez (2000), Density measurements of liquid Fe–S alloys at high pressure, *Geophys. Res. Lett.*, *27*, 811–814, doi: 10.1029/1999GL008431.

Scopigno, T., G. Ruocco, and F. Sette (2005), Microscopic dynamics in liquid metals: the experimental point of view, *Rev. Mod. Phys.*, *77*, 881–933, doi:10.1103/RevModPhys.77.881.

Seagle, C. T., A. J. Campbell, D. L. Heinz, G. Shen, and V. B. Prakapenka (2006), Thermal equation of State of Fe_3S and implications for sulfur in Earth's core, *J. Geophys. Res. Solid Earth*, *111*, 1–7, doi:10.1029/2005JB004091.

Tsujino, N., Y. Nishihara, Y. Nakajima, E. Takahashi, K. I. Funakoshi, Y. Higo, (2013), Equation of state of γ-Fe: Reference density for planetary cores, *Earth Planet. Sci. Lett.*, *375*, 244–253.

© 2017 American Geophysical Union. All rights reserved.

Accepted Article

Umemoto, K., K. Hirose, S. Imada, Y. Nakajima, T. Komabayashi, S. Tsutsui, and A. Q. R. Baron (2014), Liquid iron-sulfur alloys at outer core conditions by first-principles calculations, *Geophys. Res. Lett.*, *41*, 6712–6717, doi:10.1002/2014GL061233.

Vočadlo, L., D. Alfè, M. J. Gillan, and G. D. Price (2003), The properties of iron under core conditions from first principles calculations, *Phys. Earth Planet. Inter.*, *140*, 101–125, doi:10.1016/j.pepi.2003.08.001.

Wasson, J. T. (1974), Meteorites: Classification and Properties, Springer Science & Business Media, Berlin, Germany.

Yao, M., K. Suzuki, and H. Endo. (1980), The sound velocity of liquid Te-Se mixtures, *Solid State Commun.*, *34*, 187-189.

Zhang, L., and Y. Fei (2008), Effect of Ni on Fe-FeS phase relations at high pressure and high temperature, *Earth Planet. Sci. Lett.*, *268*, 212–218, doi:10.1016/j.epsl.2008.01.028.

Accepted Article

© 2017 American Geophysical Union. All rights reserved.

Figure captions

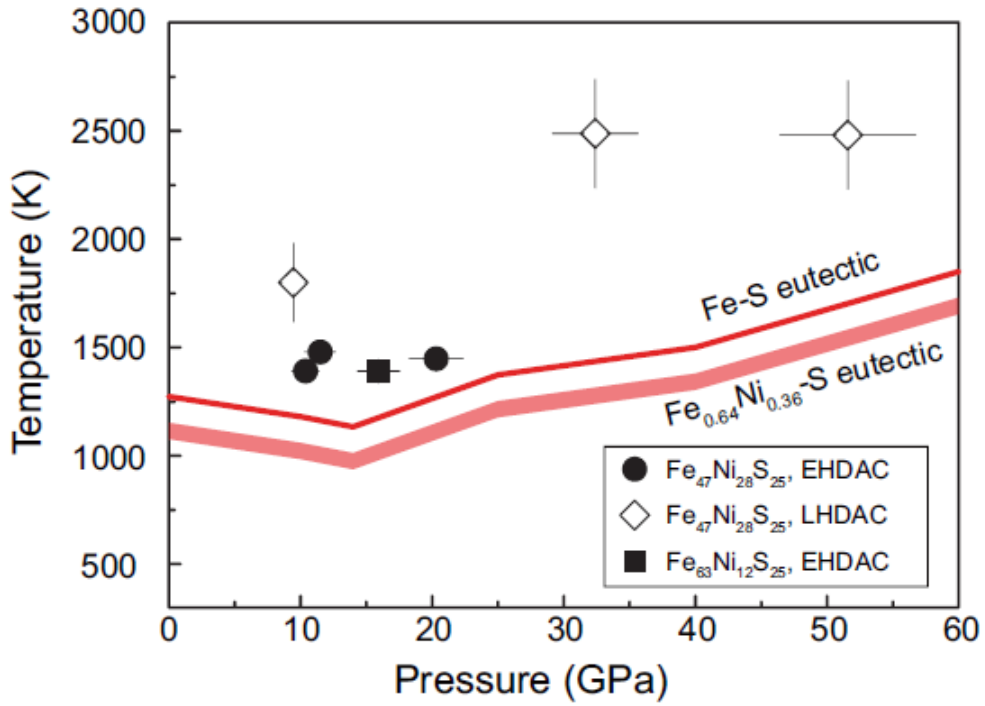

Figure 1. Eutectic melting curves in Fe–S and Fe–Ni–S systems [*Fei et al.*, 1997, 2000; *Li et al.*, 2001; *Stewart et al.*, 2007; *Zhang and Fei*, 2008; *Morard et al.*, 2007, 2008]. Closed and open symbols show our experimental *P*-*T* condition with resistance- or laser-heating DACs, respectively.

Accepted Article

© 2017 American Geophysical Union. All rights reserved.

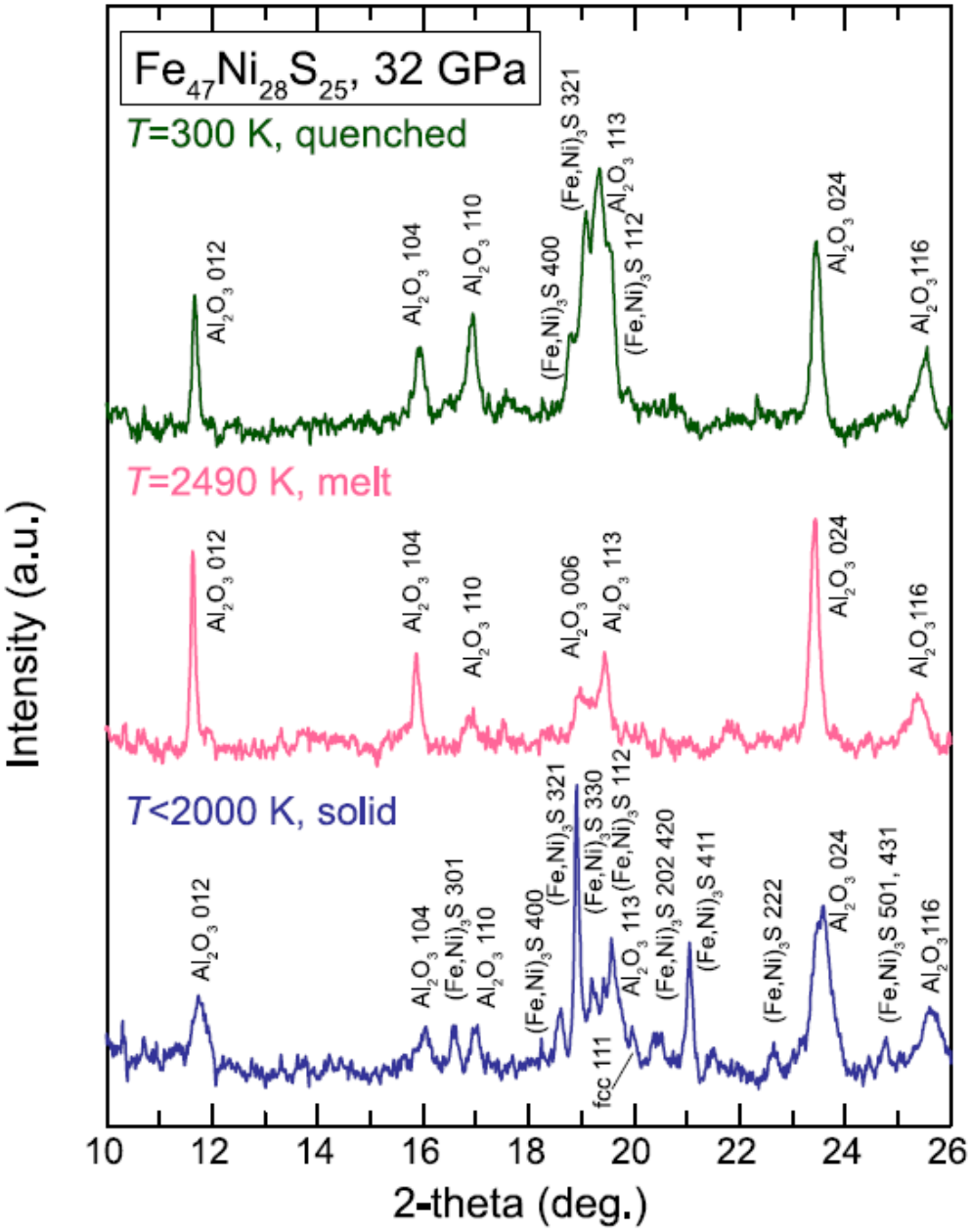

Figure 2. Typical solid, molten, and quenched XRD patterns for $(Fe,Ni)_3S$ at 32 GPa.

Accepted Article

© 2017 American Geophysical Union. All rights reserved.

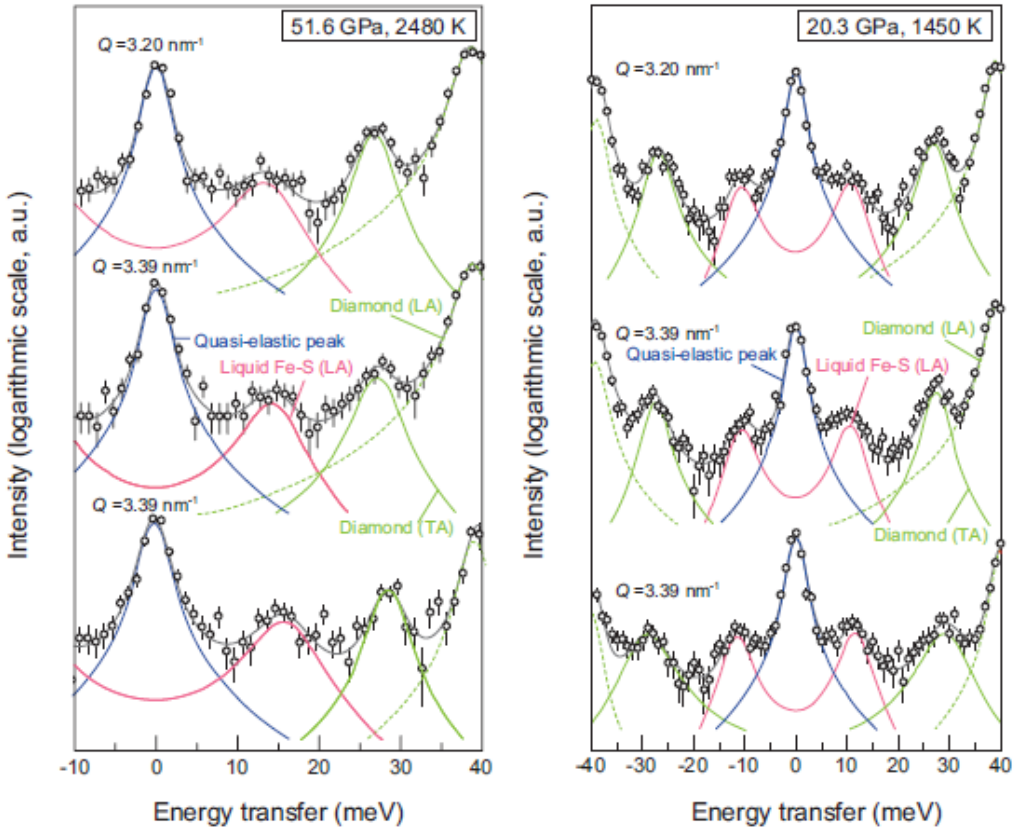

Figure 3. IXS spectra of liquid $Fe_{47}Ni_{28}S_{25}$ used for velocity determination collected at Q = 3.20 nm^{-1}, 51.6 GPa/2480 K with laser heating (a) and at Q = 3.38 nm^{-1}, 20.3 GPa/1450 K with resistance heating (b). Blue and pink lines show quasi elastic peak and longitudinal acoustic (LA) phonon peak of a liquid sample, respectively. Green solid and broken lines represent, respectively, transvers acoustic (TA) and LA phonon peaks of a diamond.

Accepted Article

© 2017 American Geophysical Union. All rights reserved.

Accepted Article

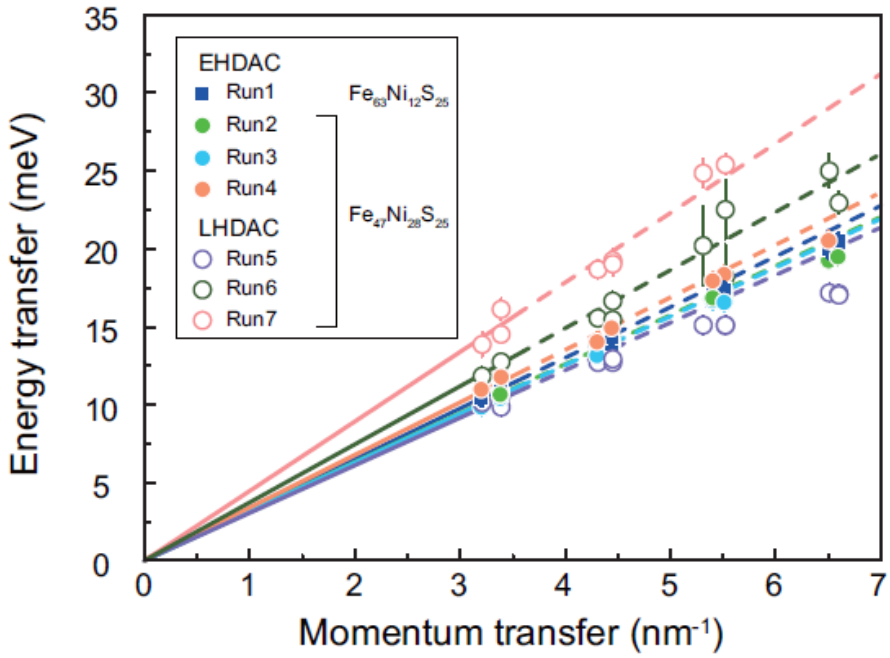

Figure 4. Phonon dispersion relations obtained in each run. Symbols are fitting results (peak positions of the LA-mode phonon peaks) from IXS spectra. The dispersion relation in this study was obtained with a line through the origin using only relatively-low Q data (Q < 3.5 nm^{-1}).

© 2017 American Geophysical Union. All rights reserved.

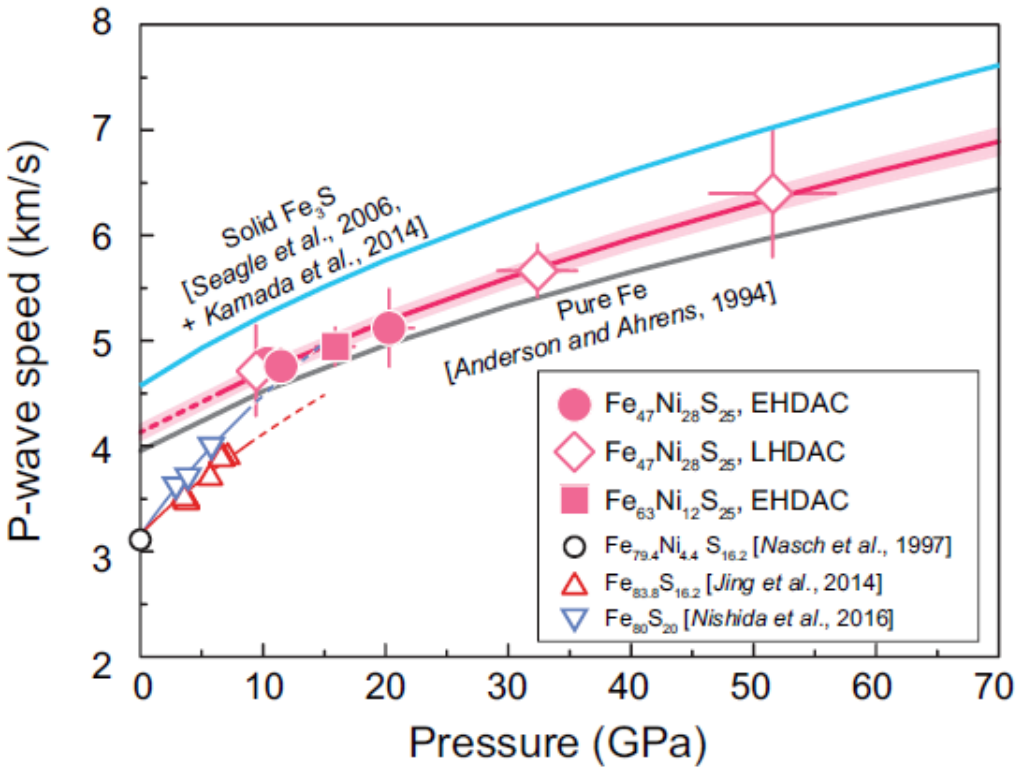

Figure 5. Sound velocities of liquid Fe–Ni–S and Fe–S alloys. Present data are shown by pink closed circles for $Fe_{47}Ni_{28}S_{25}$ in EHDAC, pink closed square for $Fe_{63}Ni_{12}S_{25}$ in EHDAC, and pink open diamonds for $Fe_{47}Ni_{28}S_{25}$ in LHDAC. Open circle is for $Fe_{79.45}Ni_{4.4}S_{16.2}$ at 1 bar [*Nasch et al.*, 1997]. Previous ultrasonic high-pressure measurements are given by open red triangles for $Fe_{84}Ni_{16}$ [*Jing et al.*, 2014] and open blue triangle for $Fe_{80}S_{20}$ [*Nishida et al.*, 2016], with their fitting curves. Grey line is for pure Fe [*Anderson and Ahrens*, 1994]. Light blue line indicates the velocity of solid Fe_3S at 2000 K calculated from those measured at room temperature [*Kamada et al.*, 2014] combined with the temperature effect on density [*Seagle et al.*, 2006].

Accepted Article

© 2017 American Geophysical Union. All rights reserved.

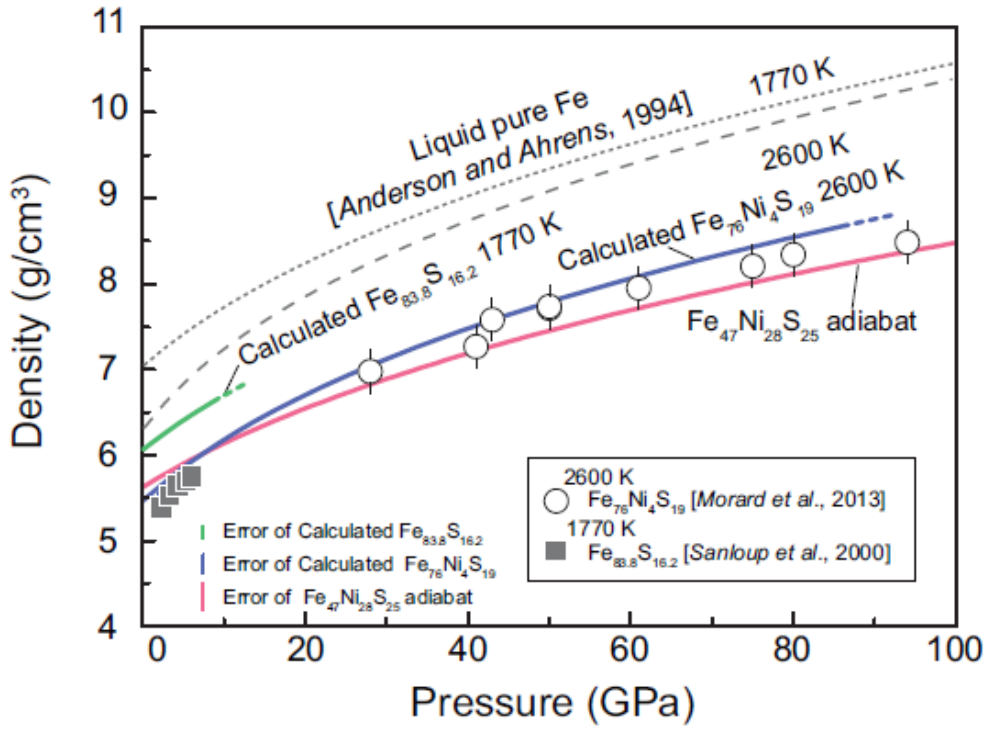

Figure 6. The adiabatic density profile for liquid $Fe_{47}Ni_{28}S_{25}$ obtained in this study (T_0 = 2000 K, solid pink curve). The isothermal density profiles of liquid $Fe_{83.8}S_{16.2}$ at 1770 K (pink dotted curve) and $Fe_{76}Ni_4S_{19}$ at 2600 K (pink dashed curve) are calculated from the present results (Eqns. 1 and 4). The density of liquid pure iron at 1770 K and 2600 K are also given by dotted and dashed gray lines, respectively. Previous measurements for liquid $Fe_{83.8}S_{16.2}$ at 1770 K [*Sanloup et al*., 2000] and $Fe_{76}Ni_4S_{19}$ at 2600 K [*Morard et al.*, 2013] are shown by closed gray squares and open circles, respectively.

Accepted Article

© 2017 American Geophysical Union. All rights reserved.

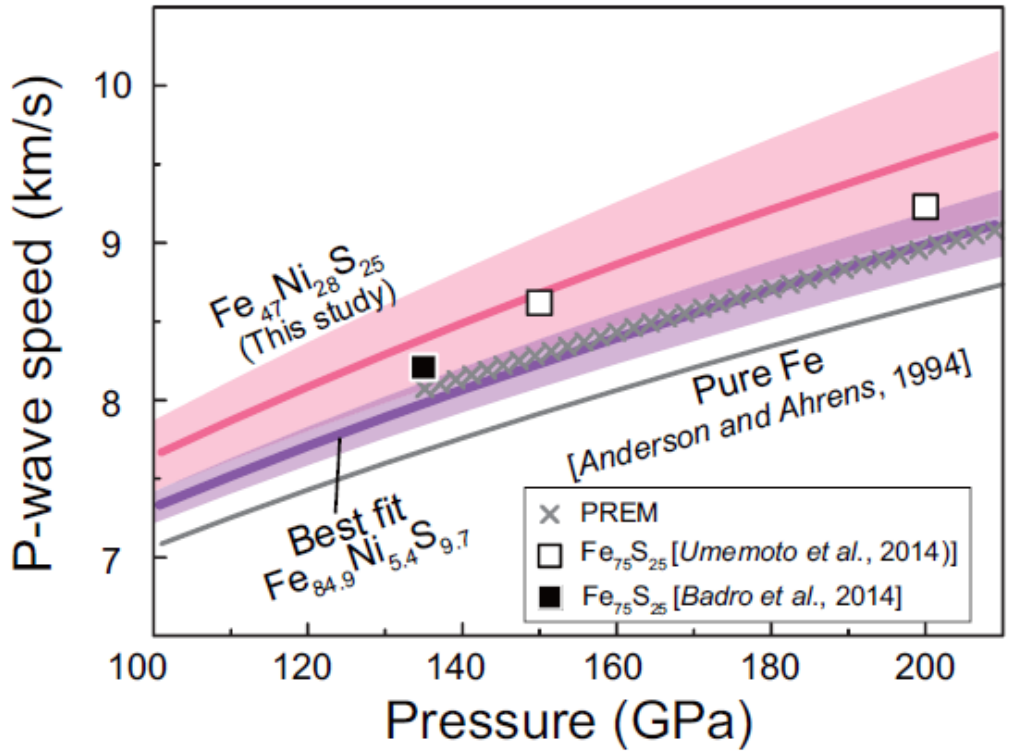

Figure 7. Sound velocities of liquid $Fe_{47}Ni_{28}S_{25}$ in this study and pure Fe [*Anderson and Ahrens*, 1994] along the adiabat with T_0 = 2000 K (dashed curve) in comparison with the PREM values (crosses). The best fit curve is for $Fe_{84.9}Ni_{5.4}S_{9.7}$ (solid pink curve). The shaded areas around curves show the uncertainties of the extrapolations (see text for detail). Open and closed squares, sound velocities of liquid $Fe_{75}S_{25}$ [*Umemoto et al.*, 2014] and $Fe_{75}S_{25}$ [*Badro et al*., 2014].

Accepted Article

© 2017 American Geophysical Union. All rights reserved.

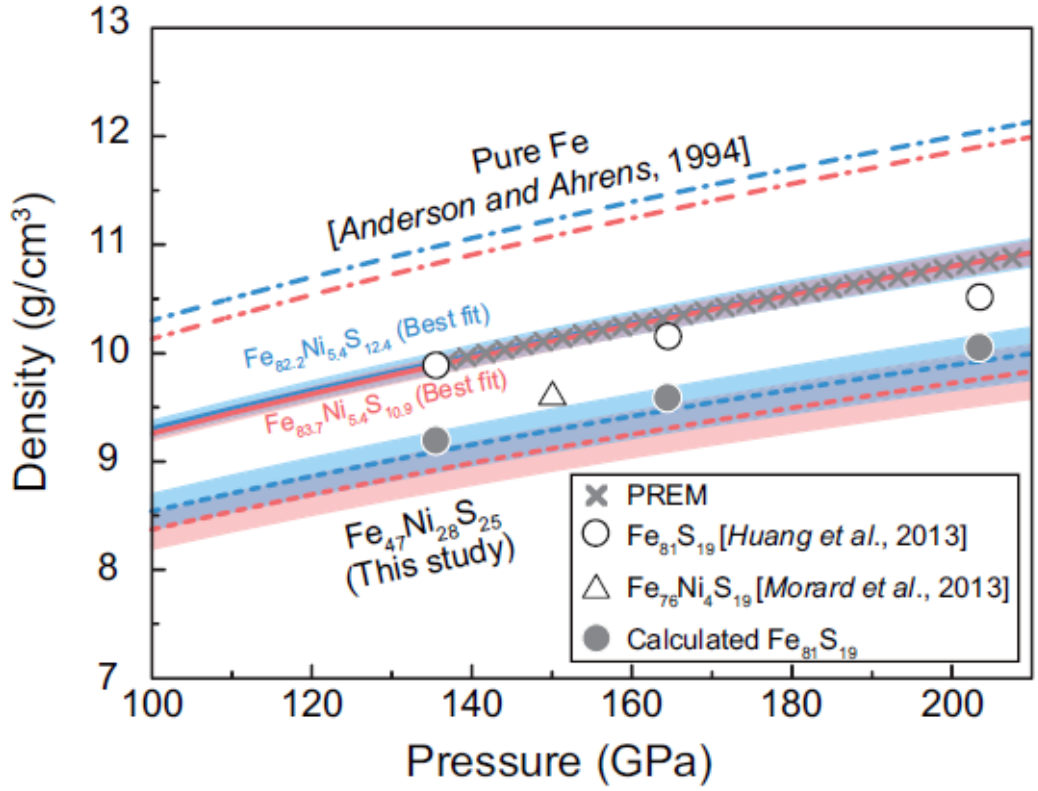

Figure 8. Density of liquid $Fe_{47}Ni_{28}S_{25}$ along adiabats with T_0 = 1880 and 2190 K (blue and red dotted curves, respectively). The density profile of pure Fe reported by *Anderson and Ahrens* [1994] is also shown. Solid blue and red curves show the best fits to the PREM (crosses) with liquid $Fe_{82.2}Ni_{5.4}S_{12.4}$ (T_{CMB} = 3600 K) and $Fe_{83.7}Ni_{5.4}S_{10.9}$ (T_{CMB} = 4300 K). Open and solid gray circles give the density of liquid $Fe_{81}S_{19}$ obtained by shock wave experiments [*Huang et al.*, 2013], and liquid $Fe_{81}S_{19}$ based on additive law by mixing the densities of $Fe_{47}Ni_{28}S_{25}$ and Fe [*Anderson and Ahrens*, 1994]. Open and solid triangles indicate liquid $Fe_{76}Ni_4S_{19}$ [*Morard et al.*, 2013]. The uncertainty in extrapolations is shown by shaded areas (see text for details).

Accepted Article

© 2017 American Geophysical Union. All rights reserved.

Accepted Article

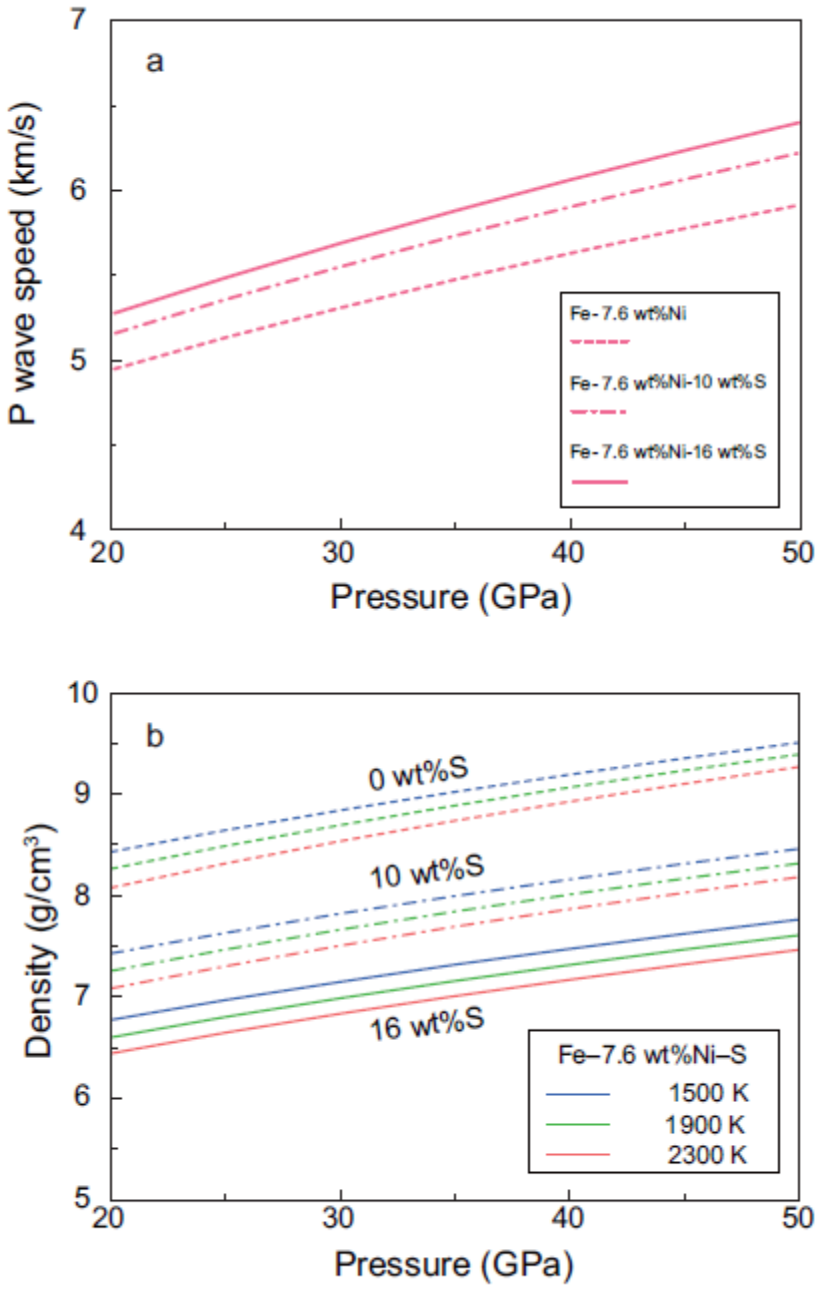

Figure 9. (a) Sound velocity and (b) Isothermal density profiles of liquid Fe–7.6wt.%Ni ($Fe_{92.7}Ni_{7.3}$, dotted line), Fe–7.6wt.%Ni–10wt.%S ($Fe_{77.0}Ni_{6.8}S_{16.2}$, broken line), and Fe–7.6wt.%–16 wt.%S ($Fe_{68.5}Ni_{6.5}S_{25}$, solid line) at 1500 K (blue), 1900 K (green) and 2300 K (red curves) in the Martian core pressure range.

© 2017 American Geophysical Union. All rights reserved.

Table 1. Experimental Condtions and Obtained Sound Velocity of Liquid $(Fe,Ni)_3S$

Run no.	Composition	Initial condition	P (GPa)	T (K)	V_P (km/s)
Resistance heating					
1	$Fe_{63}Ni_{12}S_{25}$	Synthesized	15.9(16)	1390(50)	4.94(12)
2	$Fe_{46.5}Ni_{28.5}S_{25}$	Powder mixture	10.4(10)	1390(50)	4.78(70)
3	$Fe_{46.5}Ni_{28.5}S_{25}$	Powder mixture	11.5(11)	1480(50)	4.76(80)
4	$Fe_{46.5}Ni_{28.5}S_{25}$	Synthesized	20.3(20)	1450(50)	5.12(19)
Laser heating					
5	$Fe_{46.5}Ni_{28.5}S_{25}$	Synthesized	9.5(10)	<2000[a]	4.71(30)
6	$Fe_{46.5}Ni_{28.5}S_{25}$	Synthesized	32.4(32)	2490(250)	5.66(18)
7	$Fe_{46.5}Ni_{28.5}S_{25}$	Synthesized	51.6(52)	2480(250)	6.40(31)

Numbers in parentheses indicate the pressure uncertainty in the last digits.

[a]Temperature could not be measured due to low temperature.

Accepted

© 2017 American Geophysical Union. All rights reserved.

Table 2. Fitting Results Using Murnaghan Equation of State			
T_0 (K)	K_{S0} (GPa)	K_{S0}'	ρ_0* (g/cm^3)
2000	96.1(27)	4.00(13)	5.62 (91)

* Density at 1 atm and T_0 was calculated from literature data of pure Fe [*Anderson and Ahrens*, 1994], FeS [*Nishida et al.*, 2008], and Fe–Ni alloys [*Brillo and Egry*, 2004].

Accepted Article

© 2017 American Geophysical Union. All rights reserved.